Nondissociative Adsorption of O_2 on Ge(100)

X. L. Fan,*,†,‡ W. M. Lau,‡,§,# and Z. F. Liu[||,×]

School of Material Science and Engineering, Northwestern Polytechnical University, 127 YouYi Road West, Xian, 710072, Shaanxi, China, Department of Physics, The Chinese University of Hong Kong, Shatin, Hong Kong, China, Surface Science Western, University of Western Ontario, London, Ontario, N6A 5B7, Canada, and Department of Chemistry and Centre for Scientific Modeling and Computation, The Chinese University of Hong Kong, Shatin, Hong Kong, China

Received: October 26, 2008; Revised Manuscript Received: April 2, 2009

Surface scattering experiments indicate that the dissociative chemisorption of O_2 on Ge(100) and Si(100) both proceed through precursor mediate mechanisms. The theoretical studies of O_2/Ge(100), unlike those of O_2/Si(100) that are extensive and comprehensive, have not yet been able to account for such experimental data because of the omission of the unusual triplet spin nature of the ground state of O_2. In this work we have tracked by first principles calculations the reaction paths of both triplet and singlet O_2/Ge(100) and identified several nondissociative chemisorption states that "mediate" the subsequent dissociative chemisorption of ground state O_2. In addition to explaining the experimentally observed precursor mediate routes, our computational comparison of O_2/Ge(100) and O_2/Si(100) also predicts, consistent with known experimental data, a smaller sticking coefficient for O_2/Ge(100).

Introduction

Germanium is a semiconductor and crystalline solid with importance in many areas of science and technology. Recently its importance has been further raised because its substitution for silicon has been contemplated in the manufacture of next generation metal-oxide-semiconductor field-effect transistors (MOSFETs). This is because hole and electron both run faster in germanium than in silicon.[1] There is, however, a need for research on the detailed surface oxidation processes of germanium, with the objective of optimizing the properties of oxide/semiconductor interface, the most critical component of a MOSFET. Indeed, the research effort is required because surface oxidation of germanium has not been studied in as much detail as silicon.[2] Even in the case of silicon, the theoretical research[10−13] on the initial adsorption of O_2 on Si(100) (referred to as O_2/Si(100)), which is a prototypical surface science approach to understand surface oxidation, had yielded no explanation of the experimental inference of precursor mediated adsorption[3−9]until the difference between triplet and singlet O_2 has been properly clarified with spin-specific calculations by Fan et at.[14]

In silicon-based MOSFET technology, Si(100) is chosen mainly because of the minimization of oxide−semiconductor interface states. In this context, Ge(100) should be the proper crystal surface for germanium MOSFETs because its atomic and electronic structures are similar to those of Si(100).[15−17] The adsorption of O_2/Ge(100) provides a good model system to probe the kinetics and mechanism for the optimization of the Ge MOSFET technology. In 1982, Surnev and Tikhov showed experimentally that not unlike the adsorption of O_2/Si(100), chemisorption of O_2/Ge(100) also proceeds via a precursor state.[18] Subsequently Hansen and Hudson[19,20] conducted additional molecular beam scattering measurements and further clarified that the chemisorption proceeds by two distinct mechanisms: (1) a molecular precursor-mediated mechanism predominating in the low incident kinetic energy region and (2) a direct adsorption mechanism predominating in the high kinetic energy region. In these seminal studies, the adsorption sticking coefficients were measured by the detection of the desorption of GeO, the dissociative chemisorption product, because of the high sensitivity in detecting the desorbed GeO by thermal desorption mass spectrometry. Since then, all known studies of O_2/Ge(100) have focused on dissociative chemisorption. For example, Fukuda and Ogino[21,22] employed both scanning tunneling microscopy (STM) and ultraviolet photoemission spectroscopy (UPS) to study the adsorption of O_2/Ge(100) in the exposure range of 9−200 L and temperature range from room temperature to 400 °C. At a low exposure of 9 L at room temperature, two adsorption products were detected by filled-state imaging STM as protrusions above the Ge dimer plane, together with some additional STM imaging features below the plane ("dark" in appearance). The main protrusion feature (type A) was found to be located at the center of a Ge−Ge dimer. In comparison, the minor feature (type B) was found to be located on top of one end of the dimer. The type B feature disappeared both at higher O_2 exposure at room temperature and during mild annealing. The type B feature was identified as a metastable phase, but its chemical nature was not elaborated upon except for the speculation of back-bond insertion of oxygen below one Ge atom of the Ge−Ge dimer. Unlike the type B feature, the type A feature survived both the increase in exposure and mild annealing to 300 °C. By adopting the interpretations of Uchiyama and Tsukada[23] of the adsorption of atomic oxygen on Si(100), Fukuda and Ogino[22] attributed the type A feature to a product of dissociative chemisorption with an oxygen atom on top of a Ge−Ge dimer.

* To whom correspondence should be addressed. E-mail: xlfan@nwpu.edu.cn.
† Northwestern Polytechnical University.
‡ The Chinese University of Hong Kong.
§ University of Western Ontario.
# E-mail, llau22@uwo.ca.
|| The Chinese University of Hong Kong.
× E-mail, liu@liua1.chem.cuhk.edu.hk.

10.1021/jp809480c CCC: $40.75
Published on Web 04/23/2009

Soon et al.[24] have also studied O_2/Ge(100) both experimentally and theoretically. Their density functional theory (DFT) computation approach was meticulous and thorough, but unfortunately the triplet state nature of ground state O_2 was not fully recognized. Also in this study, the adsorption of O_2 was found to be barrierless and dissociative and several distinct dissociative chemisorption states were identified. Their prediction of no nondissociative adsorption of O_2 on Ge(100) is not consistent with the experimental molecular scattering data.

In 2008, about a decade after the STM work of Fukuda and Ogino, Grassman et al.[25] revisited the structural and electronic properties of the oxidation of Ge(100) by experimental STM and theoretical DFT. The surface features previously reported by Fukuda and Ogino are confirmed by Grassman et al., who offered new interpretation of the nature of these surface features. Mainly the type A feature is proposed to be a Ge adatom being pushed outward as a result of surface oxidation. The type B feature is proposed to be either the insertion of an oxygen atom into a Ge−Ge dimer (referred therein as dimer-bridge insertion) or insertion of an oxygen atom to a back-bond (referred therein as back-bond insertion). Different from the experimental work of Fukuda and Ogino, the results of Grassman et al. indicate that the back-bond insertion can still be observed after the exposure of 100 L of O_2 at room temperature. The DFT results of Grassman et al., which are consistent with those by Soon et al., [24] also support the stability of these insertion products. Moreover, the stability of the insertion products on Ge(100) is in agreement with the stability of the insertion products in the case of O_2 /Si(100). [12] In addition to providing these additional insights into the surface features experimentally revealed by STM, Grassman et al. also show experimental evidence of Fermi level pinning on the surface with O_2 exposure at room temperature. More specifically, the Fermi level is always near the valence band maximum, no matter whether the substrate is n- or p-type. This report also shows that annealing to 325 °C does not unpin the Fermi level. Although this recent report by Grassman et al. gives an updated account of O_2/Ge(100), it still does not give any information on nondissociative O_2 adsorption on Ge(100). Further, the interpretation of the type A feature as a Ge adatom inserted into the bridge site of a Ge−Ge dimer is only inferred by the height of this feature being same as the step-height of Ge terrace on Ge(100) and by the presence of surplus Ge atoms due to surface oxidation. This interpretation needs more thorough studies.

If adsorption of O_2/Ge(100) is indeed barrierless, the adsorption should be labile and the sticking coefficient should be considerably high. However, the known sticking coefficient measurements gave no evidence of high reactivity, as the value of 0.008 is suggested to be in the low kinetic energy region, and the respective values are merely 0.018 and 0.079 for respective O_2 arrival energy at 0.09 and 0.34 eV.[18] In comparison to these sticking coefficients of O_2/Ge(100), the respective values[2] for O_2/Si(100) are 0.7 and 0.15 for O_2 arrival energy at 0.026 and 0.2 eV. Once again, these adsorption behaviors of O_2/Ge(100) have never been explained properly.

Although the spin polarized triplet state ($^3\Sigma_g^-$) of O_2 is the ground state and the singlet state ($^1\Delta_g$) is the less stable exited state with an energy gap of 0.98 eV,[26] the singlet state is commonly adopted in many theoretical studies because of the lack of proper techniques in spin-specific calculations.[10−13,24] In this paper, we report on our first principles spin-specific computational studies of O_2/Ge(100). The work adopts the known definitive and necessary inclusion of a clarification of the roles of the spin polarized triplet state ($^3\Sigma_g^-$) and the singlet state ($^1\Delta_g$) in surface oxidation. With this methodology previously developed for the examination[14] of O_2/Si(100), the potential energy surfaces of three different scenarios of O_2 approaching trajectories for both the triplet and singlet states are mapped and compared for the case of O_2/Ge(100). The justification of the selection of these trajectories has already been explained and adopted[14] in the case of O_2/Si(100).

Computational Methods

The first principles calculations of this work were carried out within the DFT method using a plane-wave basis set and Vanderbilt ultrasoft pseudopotentials[27] for the atomic core regions,[28,29] as implemented in the Vienna ab initio simulation package (VASP).[30−33] The setup was similar to that of our previous study of O_2/Si(100)[14] with a PW91 exchange correlation functional[34] and a cutoff energy of 396 eV for the plane wave expansion. The minimum energy paths for the adsorption reactions were mapped out using the nudged elastic band method developed by Jónsson and co-workers.[35,36]

The Ge(100) surface was modeled by a slab containing five atomic Ge layers and a vacuum region of 10.6 Å. Four different reconstructions of Ge(100) surface were investigated, and they included the symmetric (2×1), bucked (2×1), $p(2 \times 2)$, and $c(4 \times 2)$. Among them $c(4 \times 2)$ and $p(2 \times 2)$ are the most stable geometries. The energy difference between the two geometries is less than 0.003 eV/dimer, which agrees well with two previous studies in this topic.[37,38] Thus, the top of the slab was modeled by the $p(2 \times 2)$ surface with two asymmetric Ge dimers, while the dangling bond of the bottom Ge atoms were saturated by H atoms. After the initial structural optimization, the bottom Ge and H atoms were fixed in their bulk positions. The Brillouin zone was sampled by five special *k*-points. The *k*-points and cutoff energy were tested to give converged results. In our calculations we obtained a bond length of 1.24 Å for free O_2 in the triplet state ($^3\Sigma_g^-$) and an energy gap of 1.02 eV between $^3\Sigma_g^-$ and $^1\Delta_g$ states.

To facilitate the discussion of the impacts of the nondissociative adsorption states and pathways revealed in this work, particularly the impacts on STM studies of O_2/Ge(100) and on electronic issues such as Fermi level pinning, we also conducted band structure calculations to reveal changes in the band structure near the bandgap and in surface states. These changes were sampled with the representative nondissociative adsorption states obtained by the above potential energy surface calculations. To verify our methodology in these calculations, we have repeated the band structure and charge density distribution calculations for the clean $c(4 \times 2)$ Ge(100) surface. The results are same as those published in the literature.[39]

Results and Discussion

1. Reaction Pathways for Nondissociative Adsorption of O_2/Ge(100). The scenario analysis of the general nature of molecular oxygen arriving on Ge(100) surface can be simplified by three scenarios of O_2 approaching trajectories toward a Ge−Ge dimer, which is the most reactive part of the surface because of its π bond nature. In the first trajectory, molecular oxygen moves toward the germanium dimer with one end of O_2 attacking the up-tilted dimeric germanium atom. The results from the analysis of the reaction pathways for both triplet and singlet O_2 are summarized in Figure 1. At the very beginning of the reaction when the oxygen molecule is far from the Ge(100) surface, the triplet state is more stable than the singlet state by about 1 eV. This reflects the energy gap between the $^3\Sigma_g^-$ and the $^1\Delta_g$ states of free O_2. On the triplet potential energy

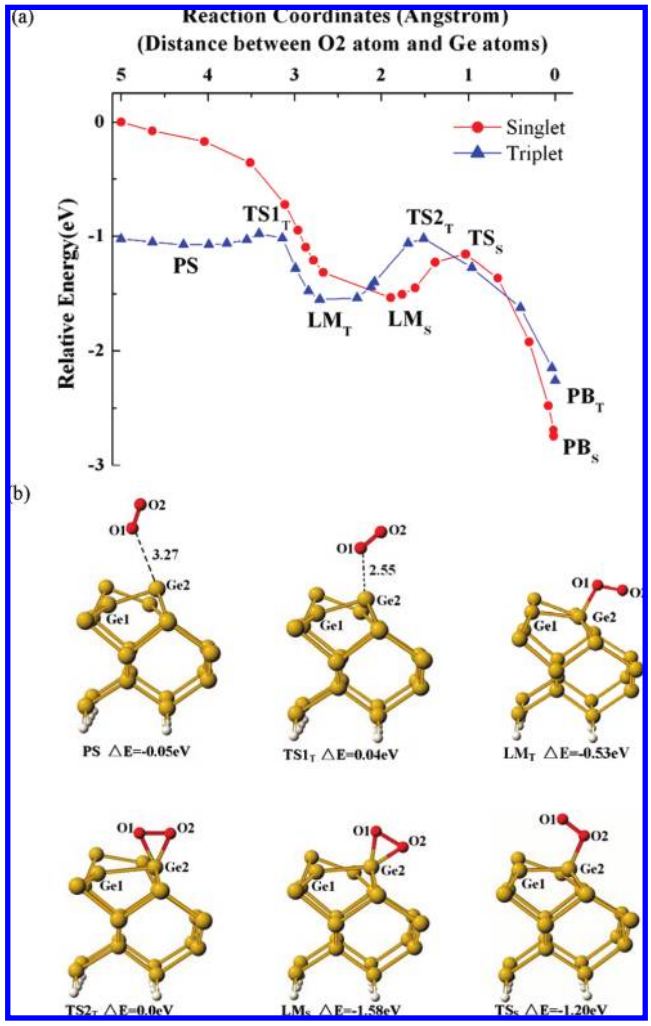

Figure 1. (a) Potential energy surface for a tilted O_2 molecule, in both triplet and singlet state, attacking the "up-tilted" Ge atom of the surface dimer. Reaction coordinates are referenced to the distances between the O2 atom and Ge2 atom before the LM state and Ge1 atom after the LM state. (b) The structures of the physisorption (PS), local minimum nondissociative chemisorption (LM), and transition state (TS), with the subscripts "T" and "S" respectively indicating the spin states of triplet and singlet.

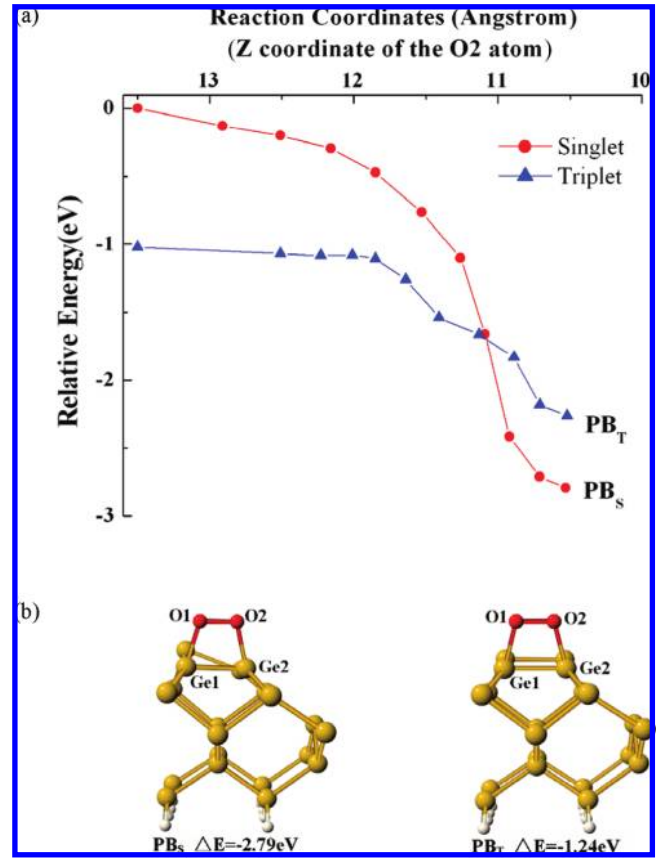

Figure 2. (a) Potential energy surface for the concerted adsorption for both the triplet and singlet O_2 when O_2 molecule is parallel to the surface and on top of a germanium dimer. Reaction coordinates are referenced to the *Z* coordinate of the O2 atom. (b) The peroxide-bridge structures of nondissociative O_2 adsorption, with the subscripts "T" and "S" respectively indicating the spin states of triplet and singlet.

surface (Figure 1a), the result shows that there exists a shallow physisorption well with the adsorption energy of 0.05 eV. The physisorbed state is labeled as PS_T. In this PS_T configuration, the lower O atom (O1) of the physisorbed oxygen molecule is 3.27 Å away from the up-tilted dimeric germanium atom (Ge2), as shown in Figure 1b. Through a barrier of 0.09 eV, the adsorption system leaves the physisorbed state, passes through the first transition state ($TS1_T$), and reaches the chemisorbed local minimum state (LM_T) with an adsorption energy of 0.53 eV. In the transition state, the distance between the O1 atom and the Ge2 atom is 2.55 Å. In the physisorbed state and first transition state, the respective distances between the oxygen molecule and the surface are 3.27 and 2.55 Å. The long bond lengths indicate that the interaction between the O_2 molecule and the surface for both the physisorbed state and first transition state are van der Waals interaction in nature. In the LM_T state, the O1 atom bonds to the Ge2 atom with a bond length of 1.96 Å, and the O−O bond slightly increases to 1.34 Å. The second oxygen atom (O2) is also drawn closer to the surface but still at a distance of 2.71 Å away from the Ge2 atom. From here, the adsorption system climbs the energy barrier of the second transition state, $TS2_T$, and reaches the next chemisorption state with further lowering in potential energy. In the $TS2_T$ configuration, both oxygen atoms are at 1.86 Å from the Ge2 atom. The relocation of O1 atom to the Ge1 atom of the Ge−Ge dimer gives rise to the formation of the peroxide-bridge chemisorption structure, which is labeled as PB_T in Figure 1. The barrier from LM_T to PB_T is 0.53 eV, and the adsorption energy of PB_T is 1.24 eV.

For the same O_2 approaching trajectory scenario, singlet molecular oxygen behaves very differently. Unlike the reaction pathway for triplet O_2, the potential energy surface for singlet O_2 drops monotonically to the first local minimum of a chemisorption state LM_S without passing through any physisorbed and transition states. The LM_S state has an O−Ge−O three-member ring structure with an adsorption energy of 1.58 eV relative to the singlet O_2 and 0.56 eV relative to the triplet O_2. For the conversion of this chemisorption local minimum to the peroxide-bridge structure, a transition state (TS_S) is identified with an energy barrier of 0.38 eV. The reaction proceeds through the transition state in which the O−Ge−O tilts to the left with an elongated O−O bond (as shown in Figure. 1) to prepare for the formation of the peroxide-bridge structure.

The second trajectory starts with the O_2 molecular axis lying above and parallel to a germanium dimer (Figure 2). In this reaction approach, the two Ge atoms of the dimer are concertedly attacked by the two O atoms. Such a reaction leads directly to the formation of the peroxide-bridge structure. In this trajectory, the potential energy curves in the singlet and triplet

TABLE 1: Calculated Geometry Parameters and Adsorption Energies for the Local Minima, Transition Structures, and Peroxide-Bridge Structures in the Triplet and Singlet States for Oxygen Molecule on Ge(100), As Shown in Figures 1 and 2[a]

	LM_T	$TS2_T$	PB_T	LM_S	TS_S	PB_S
O1−O2	1.34	1.54	1.48	1.56	1.39	1.49
Ge1−Ge2	2.57	2.93	2.45	2.84	2.54	2.45
O1−Ge2	1.96	1.86		1.81	2.55	
O2−Ge2	2.71	1.86	1.91	1.89	1.86	1.89
O1−Ge1	3.85	2.96	1.91	3.68	3.38	1.91
E_{ads} [b]	0.53	0.0	1.24	1.58	1.20	2.79

[a] Bond distance is in Å, and adsorption energy is in eV. [b] E_{ads} for the structures in the triplet state is relative to the triplet oxygen molecule, and E_{ads} for the structures in the singlet state is relative to the singlet oxygen molecule.

TABLE 2: Comparison of Calculated Adsorption Energies (in eV) of the Stable Adsorption Structures in Triplet and Singlet States for O_2/Ge(100) and O_2/Si(100)

	triplet O_2			singlet O_2		
	LM_T	IB_T	PB_T	LM_S	IB_S	PB_S
Si(100)[a]	1.61	0.34	2.78	3.02	1.56	4.14
Ge(100)	0.53	no adsorption	1.24	1.58	no adsorption	2.79

[a] Results reported in ref 14.

states are similar, and both are barrierless. Interestingly the product peroxide-bridge structure derived from the singlet state is about 0.53 eV more stable than the peroxide-bridge structure derived from the triplet state.

In the third scenario of O_2 approaching trajectory, the end of the O_2 molecule falls onto the midpoint of the germanium dimer. Interestingly, this direct insertion of O_2 into the Ge−Ge bridge site does not give any stable molecule adsorption products for both singlet and triplet O_2. In comparison, a similar scenario of O_2 approaching trajectory for the Si (100) case does lead to stable adsorption and the energy data for the "insertion-bridge" adsorption states[14] are included in Table 2 with them labeled as IB_T and IB_S. Since this trajectory approach yields no reaction on Ge(100), no further detailed discussion of this set of results is deemed illustrative and necessary, and no energy data can be included in Table 2.

In the above three possible reaction pathways, two kinds of stable molecular chemisorption configurations have been found for both triplet and singlet O_2, one with O_2 sitting on the up-tilted Ge atom and the other with O2 lying on top of the dimer. The bond distance and energy data are included in Table 1. The most stable adsorption structure in our calculations is the peroxide-bridge structure; the adsorption energy for the triplet state is 1.24 eV, whereas that for the singlet state is 2.79 eV. As shown in Figure 2, the oxygen molecule lies parallel to the surface plane with a structure like a peroxide unit having its two O atoms linking to the two Ge atoms of the Ge−Ge dimer.

It is interesting that although triplet O_2 and singlet O_2 reach these nondissociative chemisorption states via completely different potential energy surfaces and reaction pathways, their energy curves meet and cross at these states from the LM_T. As such, spin conversion can eliminate the differences of local minimum states (LM) and peroxide-bridge (PB) states between triplet and singlet O_2 in the reaction pathways. After passing these states, the adsorption system, regardless of the original spin nature of O_2, proceeds to dissociative adsorption via various competing paths which include back-bonding with the germanium atoms below the topmost dimer plane or with O atoms insertion into the dimer bridge sites. These pathways have already been adequately explained in the work of Soon et al.,[24] and similar pathways for O_2/Si(100) have also been thoroughly discussed by other groups.[12,36] Although these earlier studies ignored the difference between triplet and singlet O_2, this deficiency is no longer important after spin conversion during the residence in the nondissociative chemisorption states. As such, we will not repeat the description of the reaction pathways from nondissociative chemisorption to dissociative chemisorption.

2. Molecular Beam Scattering and STM Experimental Studies. In agreement with the calculation results of Soon et al.,[24] our results show that singlet O_2 adsorbs on the Ge(100) surface without passing through any physisorbed state or reaction barrier in the initial adsorption process. Thus, the adsorption of singlet O_2 cannot explain the known experimental observations of precursor mediated adsorption. In contrast, our computational results show that triplet O_2 reacting with Ge(100) proceeds through several nondissociative adsorption potential wells and energy barriers prior to dissociative chemisorption; hence, there are more than one "precursor" state candidate. The first "precursor" state is the shallow potential well facilitating physisorption of triplet O_2. One can understand the known experimental surface-scattering data that at low kinetic energy, an incident triplet O_2 molecule is first trapped as a physisorbed precursor. The precursor can then either desorb or climb over a reaction barrier for subsequent nondissociative chemisorption. To enter to the subsequent local minimum chemisorption well (LM_T), triplet O_2 must overcome the calculated barrier of 0.09 eV. Since the physisorption energy (0.05 eV) is smaller than this energy barrier, desorption competes favorably with chemisorption. Hence, when the kinetic energy or surface temperature is raised, the precursor-mediated mechanism becomes unimportant. The incident O_2 molecules are no longer affected by the shallow physisorption well and the smaller energy barrier against chemisorption; direct chemisorption becomes the dominating reaction pathway. It is noted that in the physisorption state and the first transition state the weak adsorption of O_2 on Ge(100) is driven by van der Waals force. Since the DFT method usually underestimates van der Waals interactions, we caution that the physisorption well and the reaction barrier from PS_T state to LM_T may well be underestimated. In fact, the respective calculated values of 0.05 and 0.09 eV are so small that both the potential well and energy barrier do not cause any observable effects in the surface scattering experiments of Hansen and Hudson which were conducted in the temperature range of 300−900 K. If the actual values are higher than these calculated values, the physisorption state (PS_T) can become important and mediate chemisorption. Further clarification of this issue will require additional calculations using a method giving more accurate van der Waals forces and by additional surface scattering experiments conducted at low temperatures.

In the context of discussing the presence of the physisorption state for the case of O_2/Ge(100), it is interesting to note that very recently Kim and Cho[40] also showed the presence of physisorption prior to chemisorption for acetic acid on Ge(100) using DFT calculations. Unlike the case of triplet O_2/Ge(100) where only one physisorption state is identified, the case of acetic acid on Ge(100) by Kim and Cho gives two physisorption states, P_H and P_C. The adsorption energy of the P_H is ~0.1 eV and is weak and similar to the physisorption state of triplet O_2/Ge(100). Interestingly, the adsorption energy of the P_C state is ~0.6 eV, which is not weak at all. In our opinion, the P_C state revealed by Kim and Cho should be described as weak chemisorption. In addition to this recent study of the adsorption

of acetic acid on Ge(100), there are two other recent studies of adsorption of organic molecules on Ge(100): pyrrole[41] and styrene.[42] In both cases, the presence of physisorption prior to chemisorption is not shown.

The second "precursor" state candidate is the LM_T state. The potential well is about 0.5 eV, and thus, the competition between trapping by and escaping from the well for a surface temperature at or above room temperature is conceivable. Obviously raising the surface temperature would increase the chance of molecular desorption. In comparison to the physisorption state (PS_T), the LM_T state is not so shallow and may be adequate in influencing the nature of O_2/Ge(100) for a substrate temperature at and above room temperature. Back to the recent work by Kim and Cho on the adsorption of acetic acid on Ge(100), the LM_T state of triplet O_2/Ge(100) has very similar adsorption energy and configuration like the P_C state revealed by Kim and Cho. In both cases, one oxygen atom of the adsorbed molecule (triplet O_2 or C═O of acetic acid) is weakly bonded to a Ge atom of the Ge−Ge dimer. For the case of O_2/Ge(100) the O−Ge distance is ∼1.9 Å. Although Kim and Cho did not give the O−Ge distance of their P_C state, we speculate that the O−Ge distance should also be close to 1.9 Å because the adsorption energy is even higher than that of the LM_T adsorption of O_2/Ge(100).

Although the second reaction trajectory shown in Figure 2 is barrierless, the probability for an oxygen molecule approaching a dimer via the second channel is much smaller than that of the first trajectory because the concerted attack requires the arrival of the molecules with a specific and small trajectory geometry window. Hence, it can only play a minor role in surface adsorption/scattering.

As mentioned earlier, Fukuda and Ogino's STM studies[21,22] of O_2/Ge(100) found a metastable adsorption product (type B feature) that only exists at the early stage of the reaction, and thus, there is unlikely to be any back-bond insertion product. The calculation results can now clearly identify the nature of surface features like this, according to the relative stability of dissociative adsorption and nondissociative adsorption structures. The type B product with a protrusion on one end of the dimer should be the nondissociative adsorption LM state in which an O_2 molecule adsorbs at one end of the dimer. Because its potential energy well is shallow, the LM state can be converted to the PB state readily. This explains the metastable nature of the type B feature in the experimental conditions of Fukuda and Ogino. The attribution of the type B feature revealed by Fukuda and Ogino to the nondissociative adsorption local minimum state also explains the absence of the same type B feature in the experimental conditions of Grassman et al.[25] Interestingly, the "type B" features found by Grassman et al. are stable such that they survive high O_2 exposure and postexposure annealing. These stability properties are not possessed by the type B of feature of Fukuda and Ogino. Because of this, we tend to agree with Grassman et al. that their "type B" features are probably the results of dissociative chemisorption, with an oxygen atom inserted into a Ge−Ge dimer or into a Ge−Ge back-bond.

Similar to the discussion of the nature of the type B feature of Fukuda and Ogino and the "type B" features of Grassman et al., we also postulate that the original type A feature of Fukuda and Ogino, an STM imaging feature of a bright protrusion at the middle of a Ge−Ge dimer, can be attributed to the PB state in Figure 2. This is a very stable nondissociative chemisorption product and should be present in both the experimental conditions employed by Fukuda and Ogino and by Grassman et al. Again, we do not disagree with Grassman et al. that some of the type A features observed by them and by Fukuda and Ogino can also be Ge adatoms which are generated by O−Ge replacement in the dissociative chemisorption processes which follow the nondissociative chemisorption processes revealed in the present work. In short, the present work provides one more choice for the interpretation of the type A features observed in the literature. The PB state also has the adsorbed oxygen located at 1.2 Å higher than the surface, same as the image height found by Grassman et al. When the PB state is annealed, it can be converted to the more stable dissociative adsorption products[12,43] or diffusively driven to the step edge to form oxygen back-bond insertion, as has been found in the case of O_2/Si(100).[44] This explanation is consistent with that of Grassman et al.

3. Changes of Surface States Induced by Nondissociative Adsorption of O_2/Ge (100). For the development of electronic devices on Ge(100) wafer surfaces, it is critical to understand the surface states in and near the bandgap because the intrinsic states of the clean Ge surface (starting from the well-known $c(4 \times 2)$ reconstructed Ge(100) surface) and extrinsic states arising from surface oxidation and other overlayer deposition processes may cause band bending, interface state formation, and Fermi level pinning. The fundamental understanding of surface states on clean Ge(100) $c(4 \times 2)$ and the conversion from the $c(4 \times 2)$ pattern to the 2×1 pattern has been nicely clarified by two very recent studies. In one of these studies Eriksson et al.[45] employed angle dependent photoemission spectroscopy (ARPES) to map the occupied surface states of $c(4 \times 2)$ and 2×1 Ge(100) surfaces and used low energy electron diffraction (LEED) to yield complementary information on the changes of surface structures in this surface phase transformation. In another study, Radny et al.[39] employed STM and DFT calculations to find the nature of surface states of Ge(100). By understanding the surface states on clean Ge(100), one can then track the changes in surface states from nondissociative O_2 adsorption, dissociative O_2 chemisorption, to oxide formation, as a step-by-step scientific investigation of the band structure and interfacial electronic properties of a three-dimensional device structure in Ge. Briefly, our local density-of-state (LDOS) calculations with 51K points along $\Gamma-J-K-J'-\Gamma-K$ symmetry direction of the $p(2 \times 2)$ surface Brillouin Zone, as shown in Figure 3a, show an occupied surface state at ∼0.1 eV below the Fermi level (labeled as S_2), several occupied bands below ∼0.4 eV (with the first band labeled as S_{up}), and a surface state at ∼0.13 eV above the Fermi level (labeled as S). As we have mentioned before, the energy difference between $p(2 \times 2)$ and $c(4 \times 2)$ is merely a few meV and they differ in the superstructure of inter-row dimer pairing. In agreement with Radny et al. our partial charge density calculations confirm that the S_{up} state is the occupied dangling bond states with charge mainly from the "up" atom of the buckled Ge−Ge dimer. In the STM experiments of Radny et al. these states are revealed by filled state imaging with sample biases from −0.4 to −0.6 V. The bias dependent imaging thus convincingly clarifies the correlation between energy location and charge density of this LDOS. Similarly, the S_2 state is the back-bond states localized primarily on the "down" atom of the Ge−Ge dimer. Finally, our results in Figure 3 also indicate that presence of a state at ∼0.13 eV above the Fermi level. Our partial charge density calculations confirm that this is the unoccupied dangling bond state contributed mainly from of the "down" atom of the Ge−Ge dimer. At low temperature, this state should be empty because it is above the Fermi level. But at an elevated temperature, some electrons from the occupied

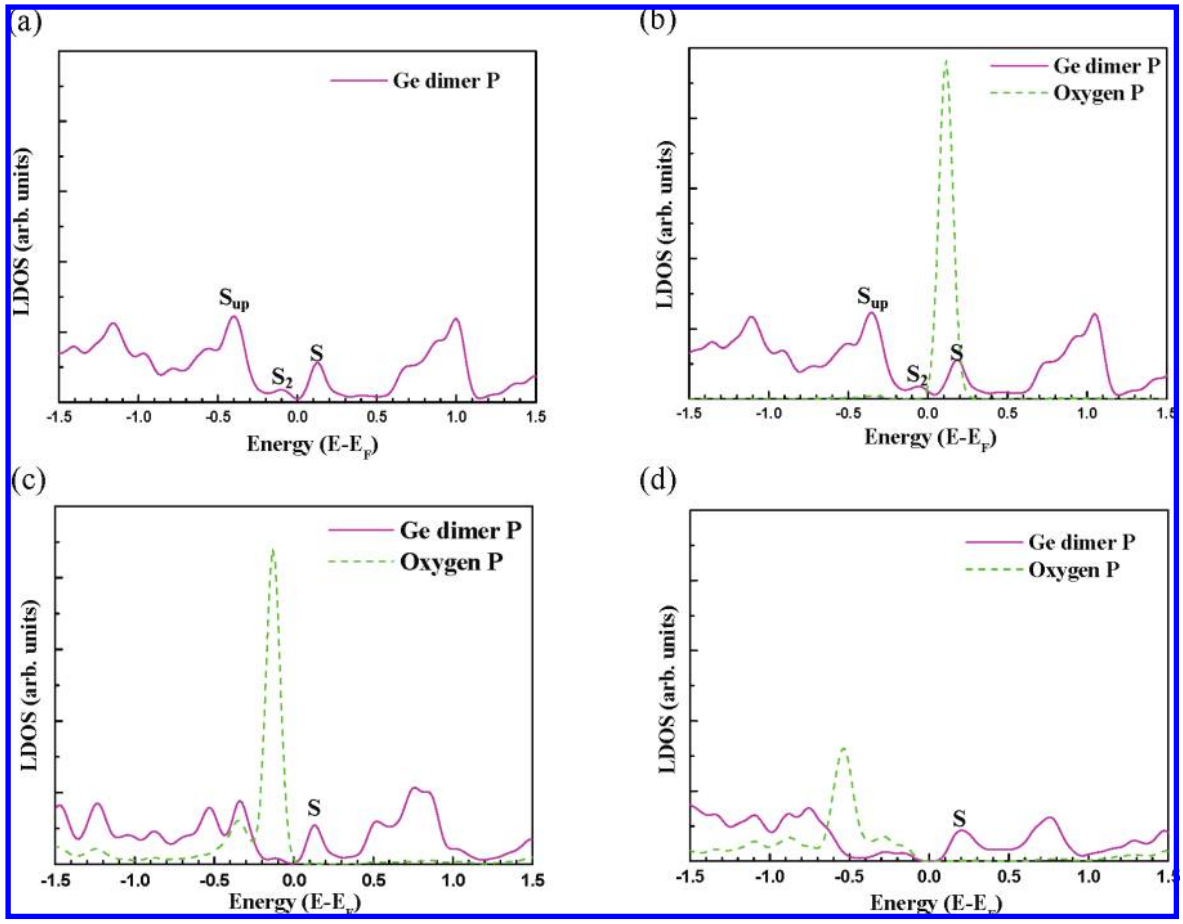

Figure 3. Local density of state (LDOS) for (a) clean $p(2 \times 2)$ Ge(100), (b) the triplet O_2 physisorption state, (c) the LM adsorption, and (d) the PB adsorption.

bands below the Fermi level can be excited to this band. Indeed, Eriksson et al. detected an ARPES peak at ~0.15 eV above the Fermi level when the Ge(100) surface is heated to above 185 K.

When triplet O_2 forms the physisorbed state on Ge(100), the results in Figure 3b show that, as expected, the surface state is almost as same as those in Figure 3a. The oxygen molecular states derived from oxygen p-orbitals are mainly localized near the Fermi level. Some electrons will likely be transferred from the occupied Ge bands to this oxygen band. Since the oxygen molecules are located much higher up than the Ge−Ge dimers on the Ge(100) surface, we predict that STM can image this physisorption state easily. Obviously the detection will require a low temperature condition for the stabilization of the weak physisorption.

For the LM adsorption, Figure 3c shows that the chemisorption of the O_2 on the "up" Ge atom of the Ge−Ge dimer changes both the S_2 and S_{up} states. In principle, STM imaging of filled states with a small bias from −0.1 to −0.2 eV will change drastically from the clean surface to the LM adsorption state. A practical problem is that the physical location of the adsorbed O_2 is near the top of the "up" Ge atom; as such, the filled state imaging may be dominated by the presence of the adsorbed O_2. The change of S_2 and S_{up} may be masked by the presence of the adsorbed O_2.

For the PB adsorption, Figure 3d shows that the relatively strong O_2−surface interactions are effective in moving almost half of the LDOS in the energy range of −1.5 to 1.5 eV, in reference to the situation in Figure 3a of the clean surface. The original S_{up} state (at −0.4 eV) disappears because of the "consumption" of the Ge dangling bonds by the PB O_2 adsorption. But the LDOS derived from the adsorbed O_2 happens to be at about −0.5 eV. Hence, we predict that filled state STM imaging will be dominated by the adsorbed O_2 at the middle of the Ge−Ge dimer. This is consistent with the observation of the type A feature by Fukuda and Ogino and later by Grassman et al. Further, we also predict that empty state STM imaging of the PB adsorption will be weak in signal strength. Because of the physical location of the adsorbed O_2 being high up above the Ge surface, the weak empty LDOS of the adsorbed O_2 above about 0.5 eV from the Fermi level will still give imaging signals. But the background signals from the Ge dimer associated with the adsorbed O_2 will be largely reduced in reference to Figure 3a of the clean surface. Indeed, Fukuda and Ogino showed that the empty state STM imaging at 0.7 V at the location of type A feature in filled state imaging gives only weak protrusion at the middle of the dimer and gives interesting dark contrast of the dimer (in comparison to the dimers that do not have any oxygen adsorption.

Among the four surface conditions in Figure 3a−d, the Fermi level of the clean Ge(100) surface is bounded by the S_2 and S states. The peaks of them are ~0.25 eV apart. Hence, although the Fermi level is not firmly pinned, the S_2 and S states must be removed before high performing electronic devices can be formed on Ge(100). The PB O_2 adsorption (Figure 3d) is certainly not yet an ideal solution, but the LDOS in −0.5 to 0.5 eV is much lower than that of the clean surface (Figure 3a) and the two surface state bands bounding the Fermi level are slightly further apart. It will be useful to track, with the same

methodology, further changes induced by dissociative adsorption and oxide formation.

4. Comparison with O_2/Si (100). Ge(100) and Si(100) surfaces exhibit the same surface reconstruction consisting of rows of buckled dimers in which two surface atoms bond to each other with a strong σ bond and a weak π bond.[15−17] Thus, we have adopted the same methodology in our recent study[14] of O_2/Si(100) to search for the optimal geometry on three different adsorption trajectories around the germanium dimer. For both O_2/Si(100) and O_2/Ge(100), the nondissociative adsorption features revealed by our computation methodology are similar, yet different. As shown by the first reaction trajectory scenario in Figure 1, the potential energy surfaces for triplet and singlet O_2 are very different; this spin state dependence is commonly found for both Ge(100) and Si(100).[14] On the potential energy surface for singlet O_2, the energy curve drops monotonically to the first local minimum of chemisorption. In comparison, the potential energy surface for triplet O_2 passes through the physisorbed precursor state and transition state before reaching the local minimum state of nondissociative adsorption. Around the first local minimum, the potential energy surface of triplet O_2 crosses that of singlet O_2. This raises an intriguing possibility that a reaction channel of spin conversion is open as the adsorbed molecule dwells on the surface and oscillates along the potential energy surface of these local potential wells. This is applicable to both Ge(100) and Si(100).

The main difference between nondissociative adsorption of O_2/Ge(100) and O_2/Si(100) is the relatively weak adsorption on Ge(100). The calculated adsorption energy results for these two cases are compared in Table 2. One sees clearly that the respective adsorption energy of the PB structure for triplet O_2/Si(100) and Ge(100) are 2.78 and 1.24 eV. For singlet O_2, they are 4.14 and 2.79 eV. The same situation also happens for the adsorption of organic molecules on Ge and Si. It is well-known that the bonding of organic molecules to Ge(100) is also much weaker than the bonding to Si(100).[46] From this alone, one would predict that the sticking coefficient on Ge(100) should be lower than that on Si(100). Obviously, the initial sticking probability is affected more by the differences in the potential energy surface along the "reaction coordinate". Both Figure 1 and Table 2 show again that the potential wells of the first local minima of the Ge(100) case are much shallower than the counterparts for the Si(100) case. Thus, O_2 may be trapped temporarily but escape easily, leading to a relatively low sticking coefficient for Ge(100).

If O_2 arrives near the middle of the surface dimer, the calculations in the present work predict no stable adsorption. In comparison, the same calculations[14] for Si(100) predicted adsorption. The prediction of no stable adsorption on Ge(100) with this O_2 approaching trajectory is reasonable because the adsorption on Ge(100) is weak in general and insertion of oxygen directly into the middle of the surface dimer is particularly energetically unfavorable. However, the probability of O_2 arrivals near this trajectory is not small, in comparison to those for O_2 arrivals with its molecular axis parallel to and on top of a surface dimer for both the cases of Ge(100) and Si(100). Consequently, the different reaction outcomes, in that adsorption proceeds on Si(100) but not on Ge(100), also imply a low sticking coefficient on Ge(100) relative to that on Si(100).

Finally, we note that in both the present study of O_2/Ge(100) and our previous study of O_2/Si(100), a perfectly ideal surface with proper reconstruction is adopted as a model surface in order to simplify the reaction considerations. In reality, oxidation of Ge(100) and Si(100) is critically affected by practical surface defects such as step edges. Indeed, the effects of step edges on oxidation of Si(100) have been examined and confirmed both experimentally and theoretically.[44]

Conclusion

Similar to the adsorption of O_2/Si(100), the precursor-mediate adsorption mechanism of O_2/Ge(100) can only be revealed by first principles calculations unless the spin state of the O_2 reactant is properly specified. This work confirms that triplet O_2 can be physisorbed and nondissociative chemisorbed on Ge(100), in agreement with the known surface-scattering experiments. The calculated bonding configurations of these adsorption states have been found to adequately clarify the interpretation of the known STM results on O_2/Ge(100). In general, the adsorption potential wells on Ge(100) are much shallower than their counterparts on Si(100). The insertion-bridge scenario of approaching trajectory yields stable adsorption on Si(100) but cannot yield stable adsorption on Ge(100). All these factors make the sticking coefficient on Ge(100) much smaller than that on Si(100).

Acknowledgment. The authors thank Professor John Hudson for his kind clarification and explanation of his original molecular beam experiments and results. This work was funded by the Discovery Grant program of the Natural Science and Engineering Research Council of Canada (NSERC) for W. M. Lau, RGC Grant 402202 for Z. F. Liu, and funds from Shannxi Province (Grant SJ08B14) for X. L. Fan. This work was also supported by the 111 Project in China. The authors also acknowledge the support from the Physics and Chemistry Departments of the Chinese University of Hong Kong and from Surface Science Western and the Faculty of Science at the University of Western Ontario.

References and Notes

(1) Dimoulas, A.; Mavrou, G.; Vellianitis, G.; Evangelou, E.; Boukos, N.; Houssa, M.; Caymax, M. *Appl. Phys. Lett.* **2005**, *86*, 032908.
(2) Yu, M. L.; Delousie, L. A. *Surf. Sci. Rep.* **1994**, *19*, 285.
(3) Ferguson, B. A.; Reeves, C. T.; Mullins, C. B. *J. Chem. Phys.* **1999**, *110*, 11574.
(4) Behringer, E. R.; Flaum, H. C.; Sullivan, D. J. D.; Masson, D. P.; Lanzendorf, E. J.; Kummel, A. C. *J. Phys. Chem.* **1995**, *99*, 12863.
(5) Miyake, T.; Soeki, S.; Kato, H.; Nakamura, T.; Namike, A.; Kanba, H.; Suzuke, T. *Surf. Sci.* **1990**, *242*, 386.
(6) Miyake, T.; Soeki, S.; Kato, H.; Nakamura, T.; Namike, A.; Kanba, H.; Suzuke, T. *Phys. Rev. B* **1990**, *42*, 11801.
(7) D'evelyn, M. P.; Nelson, M. M.; Engel, T. *Surf. Sci.* **1987**, *186*, 75.
(8) Yu, M. L.; Eldridge, B. N. *Phys. Rev. Lett.* **1987**, *59*, 1691.
(9) Memmert, U.; Yu, M. L. *Surf. Sci. Lett.* **1991**, *245*, L185.
(10) Moiyamoto, U.; Oshiyama, A. *Phys. Rev. B* **1991**, *43*, 9287.
(11) Hoshino, H.; Tsuda, M.; Oikawa, I.; Ohdomari, S. *Phys. Rev. B* **1994**, *50*, 14999.
(12) Kato, H.; Uda, T.; Terakura, K. *Phys. Rev. B* **2000**, *62*, 15978.
(13) Widjaja, Y.; Musgrave, C. B. *J. Chem. Phys.* **2002**, *116*, 5774.
(14) Fan, X. L.; Zhang, Y. L.; Lau, W. M.; Liu, Z. F. *Phys. Rev. Lett.* **2005**, *94*, 016101.
(15) Krüger, P.; Mazur, A.; Pollmann, J.; Wolfgarten, G. *Phys. Rev. Lett.* **1986**, *57*, 1468.
(16) Pollmann, J.; Krüger, P.; Mazur, A. *J. Vac. Sci. Technol. B* **1987**, *5*, 945.
(17) Krüger, P.; Pollmann, J. *Phys. Rev. Lett.* **1995**, *74*, 1155.
(18) Surnev, L.; Tikhov, M. *Surf. Sci.* **1982**, *123*, 505.
(19) Hansen, D. A.; Hudson, J. B. *Surf. Sci.* **1991**, *254*, 222.
(20) Hansen, D. A.; Hudson, J. B. *Surf. Sci.* **1993**, *292*, 17.
(21) Fukuda, T.; Ogino, T. *Phys. Rev. B* **1997**, *56*, 13190.

(22) Fukuda, T.; Ogino, T. *Appl. Surf. Sci.* **1998**, *165*, 130–132. Fukuda, T.; Ogino, T. *Appl. Phys. A* **1998**, *66*, S969.
(23) Uchiyama, T.; Tsukada, M. *Phy. Rev. B* **1997**, *55*, 9456.
(24) Soon, J. M.; Lim, C. W.; Loh, K. P.; Ma, N. L.; Wu, P. *Phys. Rev. B* **2005**, *72*, 115343.
(25) Grassman, T. J.; Bishop, S. R.; Kummel, A. C. *Surf. Sci.* **2008**, *602*, 2373.
(26) Herzberg, G. *Molecular Spectra Molecular Structure: Spectra of Diatomic Molecules*, 2nd ed.; D. van Nostrand Company Inc.: Toronto, Canada, 1950; Vol. 1.
(27) Vanderbilt, D. *Phys. Rev. B* **1990**, *41*, 7892.
(28) Cohen, M. L. *Phys. Rep.* **1984**, *110*, 293.
(29) Payne, M. C.; Teter, M. P.; Allan, D. C.; Arias, T. A.; Joannopoulos, J. D. *Rev. Mod. Phys.* **1992**, *64*, 1045.
(30) Kresse, G.; Hafner, J. *Phys. Rev. B* **1993**, *47*, R558.
(31) Kresse, G. Hafner. *J. Phys. Rev. B* **1994**, *49*, 14251.
(32) Kresse, G.; Furthmüller, J. *Phys. Rev. B* **1996**, *54*, 11169.
(33) Kresse, G.; Furthmüller, J. *Comput. Mater. Sci.* **1996**, *6*, 15.
(34) Perdew, J. P. In *Electronic Structure of Solids '91*; Ziesche, P., Eschrig, H., Eds.; Academie-Verlag: Berlin, Germany, 1991; p 11.
(35) Jónsson, H. Annu. *Rev. Phys. Chem.* **2000**, *51*, 623.
(36) Henkelman, G.; Uberuaga, B. P.; Jónsson, H. *J. Chem. Phys.* **2000**, *113*, 9901.
(37) Yoshimoto, Y.; Nakamura, Y.; Kawai, H.; Tsukada, M.; Nakayama, M. *Phys. Rev. B* **2000**, *61*, 1965.
(38) Harold, J. W. Z. *Phys. Rep.* **2003**, *388*, 1.
(39) Radny, M. W.; Shah, G. A.; Schofield, S. R.; Smith, P. V.; Curson, N. J. *Phys. Rev. Lett.* **2008**, *100*, 246807.
(40) Kim, H. J.; Cho, J. H. *J. Phys. Chem. C* **2008**, *112*, 6947.
(41) Kim, D. H.; Choi, D. S.; Hong, S. L.; Kim, S. H. *J. Phys. Chem. C* **2008**, *112*, 7412.
(42) Hwang, Y. J.; Kwang, E. K.; Kim, D. H.; Kim, A. S.; Hong, S. L.; Kim, S. H. *J. Phys. Chem. C* **2009**, *113*, 1426.
(43) Watanabe, H.; Kato, K.; Uda, T.; Fujita, K.; Ichikawa, M. *Phys. Rev. Lett.* **1998**, *80*, 345.
(44) Chung, C. H.; Yeom, H. W.; Yu, B. D.; Lyo, I. W. *Phys. Rev. Lett.* **2006**, *97*, 036103.
(45) Eriksson, P. E. J.; Adel, M.; Sakamoto, K.; Uhrberg, R. I. G. *Phys. Rev. B* **2008**, *77*, 085406.
(46) Cho, J. H.; Kim, K. S.; Morikawa, Y. *J. Chem. Phys.* **2006**, *124*, 024716.

JP809480C